IEICE TRANSACTIONS

on Communications

VOL. E101-B NO. 2
FEBRUARY 2018

A PUBLICATION OF THE COMMUNICATIONS SOCIETY

The Institute of Electronics, Information and Communication Engineers
Kikai-Shinko-Kaikan Bldg., 5-8, Shibakoen 3chome, Minato-ku, TOKYO, 105-0011 JAPAN

IEICE TRANS. COMMUN., VOL.E101–B, NO.2 FEBRUARY 2018

PAPER Special Section on Recent Progress in Antennas and Propagation in Conjunction with Main Topics of ISAP2016

Inter-Terminal Interference Evaluation of Full Duplex MIMO Using Measured Channel

Yuta KASHINO[†a)], **Masakuni TSUNEZAWA**[†], ***Student Members***, **Naoki HONMA**[†], ***and*** **Kentaro NISHIMORI**[††], ***Members***

SUMMARY In-band full-duplex (FD) Multiple-Input and Multiple-Output (MIMO) communication performs uplink and downlink transmission at the same time using the same frequency. In this system, the spectral efficiency is theoretically double that of conventional duplex schemes, such as Time Division Duplex (TDD) and Frequency Division Duplex (FDD). However, this system suffers interference because the uplink and downlink streams coexist within the same channel. Especially at the terminal side, it is quite difficult for the terminal to eliminate the interference signals from other terminals since it has no knowledge about the contents of the interference signals. This paper presents an inter-terminal interference suppression method between the uplink and downlink signals assuming the multi-user environment. This method uses eigen-beamforming at the transmitting terminal to direct the null to the other terminal. Since this beamforming technique reduces the degrees of freedom available, the interference suppression performance and transmitting data-rate have a trade-off relation. This study investigates the system capacity characteristics in multi-user full-duplex MIMO communication using the propagation channel information measured in an actual outdoor experiment and shows that the proposed communication scheme offers higher system capacity than the conventional scheme.

key words: *MIMO, full duplex, interference reduction, inter-terminal interference*

1. Introduction

One of the important issues in wireless communication is increasing the capacity within the constraints of the limited spectral resources [1]. Hence, the future wireless system is required to achieve higher spectral efficiency than current systems. To satisfy this requirement, in-band full duplex (FD) communication [2]–[4] is being studied. Current and conventional systems use Frequency Division Duplex (FDD) or Time Division Duplex (TDD) scheme. FDD requires two separate frequency bands for uplink and downlink transmissions. TDD requires only a single frequency band and the uplink and downlink connections share the same channel but in different periods. This may cause a reduction in communication speed because the transmitter and the receiver are not operated at the same time.

To solve these problems, in-band FD multiple-input and multiple-output (MIMO) communication is being studied [5], [6]. The FD scheme is expected to double the frequency utilization efficiency compared with conventional duplex schemes such as FDD and TDD, because the FD scheme uses the same frequency channel to realize simultaneous uplink and downlink transmission. As pointed out in the above references, self-interference suppression is a key challenge in the FD scheme because the receiver is affected by the significantly strong signal transmitted from the station's own transmitting antenna. Study [5] uses various kinds of techniques, both analog and digital, and interference cancellation of more than 100 dB was realized. Also, the antenna arrangement can be exploited for self-interference cancellation [7], and the authors have extended this idea to MIMO systems [8]. However, none of these techniques are suitable for mobile terminals because they require highly complex or bulky hardware for achieving high interference cancelation performance.

One solution to this problem is the unidirectional FD scheme [9]. In this scheme, only the base station or the relay station performs simultaneous transmission and reception. Even though the terminal station does not perform simultaneous transmission and reception, the spectral efficiency is doubled because the uplink and the downlink communication are realized at the same time without extending the bandwidth. Accordingly, the RF front end used in the current mobile handsets can be used because no simultaneous transmission and reception is performed at the terminal. However, there is a problem that interference occurs between the terminals because transmitting terminals will coexist with receiving terminals. A solution must be found in the physical layer because it is very difficult to reconstruct the desired signal because the interference distorts and adds noise to the signal. Moreover, the knowledge of the contents of the interference signal from the other terminal is not available at the receiving terminal, which makes it difficult to solve the problem.

This paper focuses on the inter-terminal interference and proposes an inter-terminal interference suppression method to improve the system capacity including uplink and downlink users. The proposed method uses eigen-beamforming at the transmitting side, as this renders it unnecessary for the receiving terminal to acquire any priori information. However, the transmission capacity is degraded because some array degrees of freedom are consumed by null-beamforming. Since the necessary degrees of freedom for null-beamforming depend on the environment between

Manuscript received February 15, 2017.
Manuscript revised June 15, 2017.
Manuscript publicized August 22, 2017.

[†]The authors are with the graduate school of Engineering, Iwate University, Morioka-shi, 020-8551 Japan.
[††]The author is with the Faculty of Engineering, Niigata University, Niigata-shi, 950-2181 Japan.
a) E-mail: t2316012@iwate-u.ac.jp

DOI: 10.1587/transcom.2017ISP0025

the transmitting and receiving terminals, this needs to be clarified in actual environments. Accordingly, we carried out a channel measurement campaign, and the feasibility of the proposed FD scheme was confirmed.

In the remainder of this paper, 2 explains the principle of the proposed method, while 3 and 4 show experimental conditions and results, respectively.

2. Interference Suppression Method by Eigenbeamforming

2.1 Proposed System Model

Figure 1 shows the system model considered in this study. Although there may be many users communicating in the coverage area of the BS, just two users are considered in this FD scenario. User selection and scheduling are not taken into consideration for simplicity because we focus on the fundamental performance of the FD system. Although estimating and sharing the time-varying channel information is an important problem, this study assumes that the channel information is already known at all stations. These problems are quite important and they will be resolved in future work. This system model assumes the following situation: uplink user terminal 1 (UT1) and downlink user terminal 2 (UT2) communicate with the BS (Base Station) at the same time. The BS employs separate transmitting and receiving antennas to enable simultaneous communication through uplink channel $\boldsymbol{H}_1$ and downlink channel $\boldsymbol{H}_2$; perfect self-interference elimination inside the BS is assumed. This assumption is quite important because the focus of this paper is inter-terminal interference. The signal transmitted from UT1 reaches UT2 via the interference channel, $\boldsymbol{H}_\mathrm{i}$. Though this scheme alleviates the intense self-interference inside the UTs, the transmitted signal for one UT interferes with the other UT. To solve this problem, this study adopts an eigen-beamforming technique at the transmitting UT, i.e. UT1 directs a null to UT2. The capacity improvement due to the proposed scheme is evaluated using a propagation channel measured in an actual outdoor environment.

2.2 Eigen-Beamforming Method

First, we describe the eigen-beamforming method used for interference suppression. Figure 2 shows the concept of eigen-beamforming. The inter-terminal interference channel matrix is defined as,

$$\boldsymbol{H}_\mathrm{i} = \begin{bmatrix} h_{\mathrm{i},11} & \cdots & h_{\mathrm{i},1N_1} \\ \vdots & \ddots & \vdots \\ h_{\mathrm{i},N_2 1} & \cdots & h_{\mathrm{i},N_2 N_1} \end{bmatrix}, \tag{1}$$

where the size of the matrix is $N_2 \times N_1$ when the numbers of antennas of the uplink and downlink terminals are N_1 and N_2, respectively, see Fig. 2. Singular value decomposition of $\boldsymbol{H}_\mathrm{i}$ can be expressed as,

$$\boldsymbol{H}_\mathrm{i} = \boldsymbol{U}_\mathbf{i}\boldsymbol{\Sigma}_\mathbf{i}\boldsymbol{V}_\mathbf{i}^{H}. \tag{2}$$

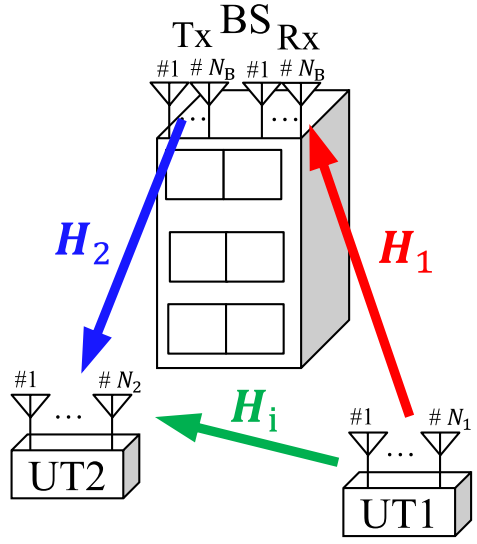

Fig. 1 Proposed system model.

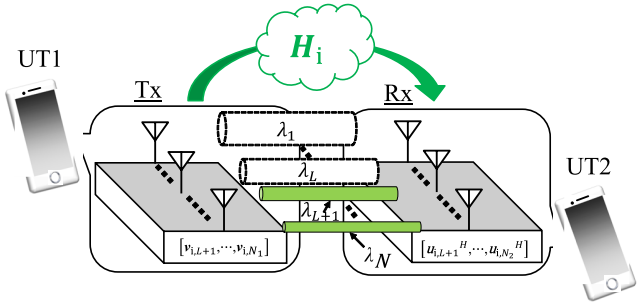

Fig. 2 Conceptual diagram of eigen-beamforming.

In the above equation, $\boldsymbol{U}_\mathrm{i}$ and $\boldsymbol{V}_\mathrm{i}$ are singular vector matrices, and $\boldsymbol{\Sigma}_\mathrm{i}$ is a singular value matrix. $\{\cdot\}^H$ represents the complex conjugate transpose of the matrix. Also, the maximum number of eigenvalues, N, in $\boldsymbol{H}_\mathrm{i}$ is defined as,

$$N = \min(N_1, N_2). \tag{3}$$

The singular vector matrix of (2) is expressed as,

$$\boldsymbol{U}_\mathbf{i} = [\boldsymbol{u}_{\mathrm{i},1}, \cdots, \boldsymbol{u}_{\mathrm{i},N_2}] \tag{4}$$

$$\boldsymbol{\Sigma}_\mathbf{i} = \mathrm{diag}(\sqrt{\lambda_{\mathrm{i},1}}, \cdots, \sqrt{\lambda_{\mathrm{i},N}}) \tag{5}$$

$$\boldsymbol{V}_\mathbf{i} = [\boldsymbol{v}_{\mathrm{i},1}, \cdots, \boldsymbol{v}_{\mathrm{i},N_1}]. \tag{6}$$

$\lambda_{\mathrm{i},1}, \cdots, \lambda_{\mathrm{i},N_\mathrm{i}}$ is a list of eigenvalues arranged in descending order. Also, interference power P_i through $\boldsymbol{H}_\mathrm{i}$ is written as

$$\begin{aligned} P_\mathrm{i} &= ||\boldsymbol{H}_\mathrm{i}||_F^2 \frac{P_{\mathrm{t}1}}{N_1} \\ &= (\lambda_{\mathrm{i},1} + \cdots + \lambda_{\mathrm{i},N}) \frac{P_{\mathrm{t}1}}{N_1}. \end{aligned} \tag{7}$$

where $||\cdot||_F$ represents the Frobenius norm, and $P_{\mathrm{t}1}$ is the total transmitting power at UT1. In this beamforming scheme, some of the column vectors in the singular vector matrix, $\boldsymbol{V}_\mathbf{i}$, are used for transmitting weight. When L degrees of freedom are used for interference suppression, the interference

is minimized by choosing the L vectors corresponding to the lowest L eigenvalues. Hence, the transmitting weight vector is expressed as,

$$\boldsymbol{V}_{\mathrm{i}}{}^{(N-L)} = [\boldsymbol{v}_{\mathrm{i},L+1}, \cdots, \boldsymbol{v}_{\mathrm{i},N_1}]. \tag{8}$$

The receiving vectors corresponding to this transmitting weight are written as,

$$\boldsymbol{U}_{\mathrm{i}}{}^{(N-L)} = [\boldsymbol{u}_{\mathrm{i},L+1}, \cdots, \boldsymbol{u}_{\mathrm{i},N_2}]. \tag{9}$$

Note that the receiving weight is not used in an actual system, but is defined here just to simplify the following discussion. Applying these weights, self-interference channel $\boldsymbol{H}_{\mathrm{i}}$ is converted into the equivalent inter-terminal interference channel $\boldsymbol{H}_{\mathrm{i}}{}^{(N-L)}$ expressed as,

$$\begin{aligned}\boldsymbol{H}_{\mathrm{i}}{}^{(N-L)} &= \boldsymbol{U}^{(N-L)H}\boldsymbol{H}_{\mathrm{i}}\boldsymbol{V}^{(N-L)} \\ &= \mathrm{diag}(\sqrt{\lambda_{\mathrm{i},L+1}}, \cdots, \sqrt{\lambda_{\mathrm{i},N}}),\end{aligned} \tag{10}$$

where the number of streams in this case is $N - L$. When this transmitting weight is used, the interference power given by,

$$\begin{aligned}P_{\mathrm{i}}{}^{(L-N)} &= ||\boldsymbol{H}_{\mathrm{i}}{}^{(N-L)}||_F^2 \frac{P_{\mathrm{t1}}}{N_1} \\ &= (\lambda_{\mathrm{i},L+1} + \cdots + \lambda_{\mathrm{i},N})\frac{P_{\mathrm{t1}}}{N_1}.\end{aligned} \tag{11}$$

By using the transmitting weight mentioned above, the interference power at the receiver becomes smaller than (7). Using the lower-ranked eigenvectors as the transmitting weight makes it possible to suppress the interference power. However, this reduces the maximum possible number of streams at the transmitting terminal, which may degrade the transmission capacity. In this study, we consider the effect of the reduced number of degrees of freedom on the transmission capacity characteristics.

3. Experimental Conditions and Experimental Environment

Figure 3 shows the base station antennas and user terminal antennas used in this measurement. In this measurement campaign, the center frequency was set to 2.47125 GHz. This experiment assumed that the two terminals simultaneously communicate with the base station. The base station antenna consists of four subarrays, each of which has four-element vertical patch antennas, where the signals at all elements are combined through the feedlines with identical phase delays. In the FD scheme, the number of BS antennas is four, and same BS antennas are used in measuring both $\boldsymbol{H}_1$ and $\boldsymbol{H}_2$. Each terminal has a four-element sleeve linear array, where the inter-element spacing is set to 0.5 λ (λ: wavelength in a vacuum).

Figure 4 shows the measurement environment and route. In this photo, point A is 65 m away from point C, which is just under the building mounting the BS, and point B lies midway between them. UT2 was located at point C or point D. All channels existing among the BS, UT1, and

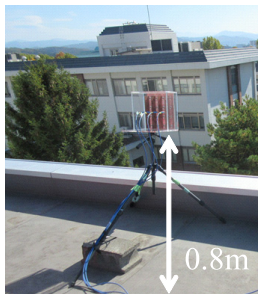

Above ground clearance
About 16m

(a) Base station antennas

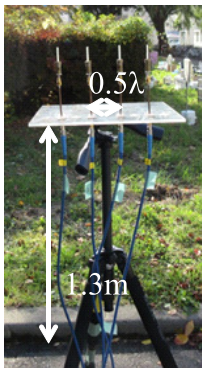

(b) Users terminal antenna

Fig. 3 Antennas used.

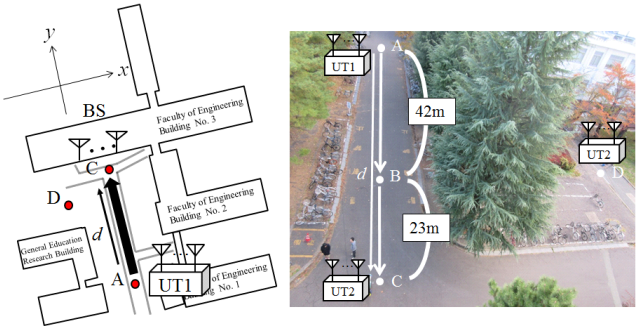

Fig. 4 Measurment route.

UT2 ($\boldsymbol{H}_1$, $\boldsymbol{H}_2$, $\boldsymbol{H}_{\mathrm{i}}$) were measured while UT1 was moved from point A to point C by way of point B. Also, the array orientations of the user terminals were set on either the x or y direction as shown in Fig. 4.

4. Results

4.1 Eigenvalue Distribution

Figure 5 shows the eigenvalue characteristics of two different channels versus UT1 location, which is measured by d (the distance from point C) ; UT2 remains fixed at point C. Result (a) shows the eigenvalues of the channel between BS and UT1, and (b) shows the eigenvalues of the channel between UT1 and UT2. These figures show that the average difference between the first eigenvalue and the second eigenvalue is 16.8 dB and 12.6 dB for BS-UT1 and UT1-UT2, respectively. Hence, the eigenvalues (other than the first one in the interference channel between UT1 and UT2) remain relatively higher than that between BS and UT1. The reason for this is that the effect of multipath propagation is more intense between two ground-level sites than that from a low site to the BS, whose elevation is much higher than ground level.

4.2 Eigenvalue Criteria: Achievable Rate Definition

In this evaluation the number of antennas at all stations are

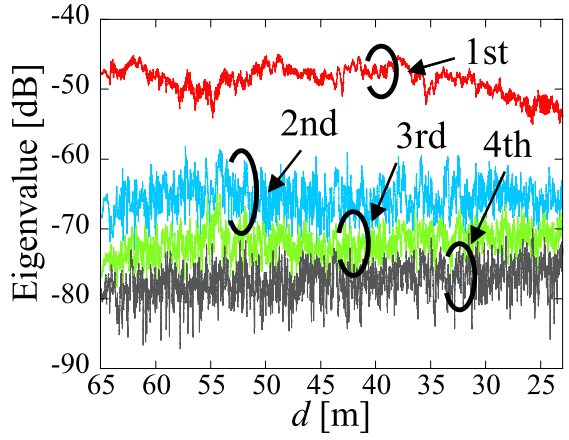

(a)Between BS-UT1

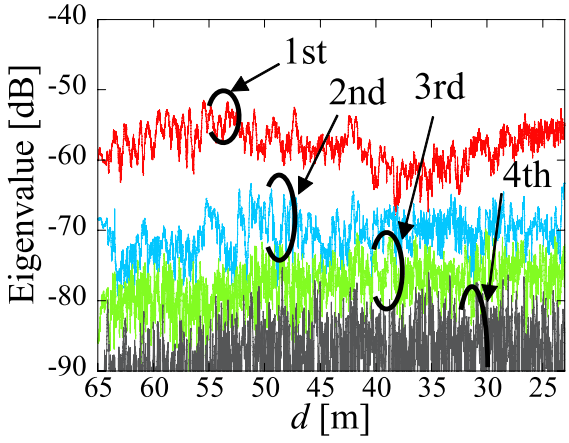

(b)Between UT1-UT2

Fig. 5 Distance characteristics of eigenvalue distribution.

identically given as $N_1 = N_2 = N_B = M$, and the transmitting power at all stations are also identical as P_t for simplicity. This assumption is fair because the transmission power is limited by RF frontend performance, and all stations are assumed to have the same RF frontends in this study.

The transmission capacity was calculated using the following equations,

$$C_1 = \log_2 \left| \boldsymbol{I} + \boldsymbol{H}_1 \boldsymbol{H}_1{}^H \frac{P_t}{M\sigma_n^2} \right| \tag{12}$$

$$C_2 = \log_2 \left| \boldsymbol{I} + \boldsymbol{H}_2 \boldsymbol{H}_2{}^H \frac{P_t}{M\sigma_n^2} \right| \tag{13}$$

$$C_{TDD} = \frac{1}{2}(C_1 + C_2) \tag{14}$$

$$C_{MU-MIMO} = \log_2 \left| \boldsymbol{I} + \boldsymbol{H}_M \boldsymbol{H}_M{}^H \frac{P_t}{M\sigma_n^2} \right| \tag{15}$$

$$C_{1BF} = \log_2 \left| \boldsymbol{I} + (\boldsymbol{H}_1 \boldsymbol{V}_i{}^{(N-L)})(\boldsymbol{H}_1 \boldsymbol{V}_i{}^{(N-L)})^H \frac{P_t}{M\sigma_n^2} \right| \tag{16}$$

$$C_{2BF} = \log_2 \left| \boldsymbol{I} + (\boldsymbol{H}_2{}^T \boldsymbol{U}_i{}^{(N-L)^*})(\boldsymbol{H}_2{}^T \boldsymbol{U}_i{}^{(N-L)^*})^H \frac{P_t}{M\sigma_n^2} \right| \tag{17}$$

Table 1 Summary of the signal flow and capacity.

	Period 1		Period 2		Capacity
	UT1	UT2	UT1	UT2	
TDD	Uplink	-	-	Downlink	Eq. (14)
MU-MIMO	Downlink	Downlink	Downlink	Downlink	Eq. (15)
FD	Uplink	Downlink	Downlink	Uplink	Eqs. (16)–(19)

$$C_{2i} = \log_2 \left| I + \left(\boldsymbol{H}_2 \boldsymbol{H}_2{}^H \frac{P_t}{M\sigma_n^2} \right) \cdot \left\{ \boldsymbol{I} + (\boldsymbol{H}_i \boldsymbol{V}_i{}^{(N-L)})(\boldsymbol{H}_i \boldsymbol{V}_i{}^{(N-L)})^H \frac{P_t}{M\sigma_n^2} \right\}^{-1} \right| \tag{18}$$

$$C_{1i} = \log_2 \left| I + \left(\boldsymbol{H}_1{}^T \boldsymbol{H}_1{}^* \frac{P_t}{M\sigma_n^2} \right) \cdot \left\{ \boldsymbol{I} + (\boldsymbol{H}_i \boldsymbol{U}_i{}^{(N-L)^*})(\boldsymbol{H}_i \boldsymbol{U}_i{}^{(N-L)^*})^H \frac{P_t}{M\sigma_n^2} \right\}^{-1} \right|, \tag{19}$$

where σ_n^2 is the noise power, $\{\cdot\}^*$ represents conjugate operation, and C_1 and C_2 represent the raw uplink and downlink capacities without any interference and beamforming. $\boldsymbol{V}_i^{(N-L)}$ and $\boldsymbol{U}_i^{(N-L)}$ represent the eigenvectors corresponding to $(N-L+1)$th$\sim N$th eigenmodes. Although C_1 and C_2 represent UT1 uplink and UT2 downlink capacities, respectively, UT1 downlink and UT2 uplink capacities are identical to C_1 and C_2, respectively due to the channel capacity duality [10]. C_{TDD} represents the TDD system capacity when the burst period is equally shared by uplink and downlink. $C_{MU-MIMO}$ is the downlink capacity with block diagonalization (BD) based multi-user (MU) MIMO [11], [12], where BS uses a four element subarray and each UT uses two eigenmodes corresponding to the two highest eigenvalues. $\boldsymbol{H}_M$ represents the channel when BD-based weight is applied at both transmitter and receiver sides. The weight determination method is detailed in Appendix. C_{FD} is the system capacity using the proposed FD scheme. The signal flow and capacity are summarized in Table I.

Since the proposed FD scheme has two periods to realize the bidirectional communication between the BS and UTs, the capacities with periods 1 and 2 are averaged as,

$$C_{FD} = \frac{1}{2}(C_{1BF}(\mathrm{UL}) + C_{2i}(\mathrm{DL}) + C_{2BF}(\mathrm{UL}) + C_{1i}(\mathrm{DL})). \tag{20}$$

C_{1BF}, C_{2BF}, C_{1i}, and C_{2i} are the partial capacities that are used for calculating the proposed FD system capacity [13], C_{FD}. When UT1 and UT2 are the uplink and downlink users at a certain moment, the uplink and downlink capacities are expressed as C_{1BF} and C_{2i}, respectively, and the system capacity at this moment is defined as the sum of them. L indicates the number of freedom used for forming nulls at the uplink terminal, where the capacity without beamforming is calculated by setting $L = 0$. UT1 uses L degrees of freedom for nulling, so C_{1BF} is reduced by the number of nulls. Though UT2 is receiving the signal from the BS, the remaining interference from UT1 impacts the capacity of UT2 as C_{2i}. At the next moment, UT1 and UT2 become the

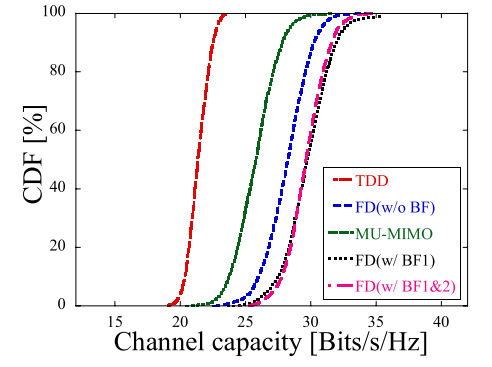

(a)Array facing in the x axis direction

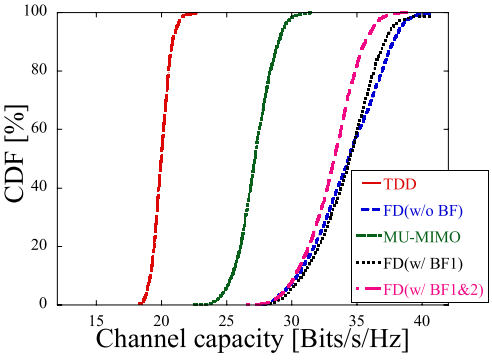

(b)Array facing in the y axis direction

Fig. 6 CDF of channel capacity between A-B.

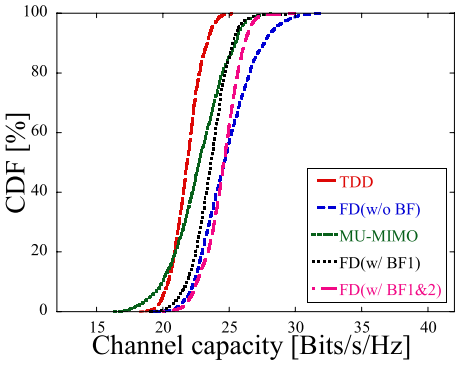

(a)Array facing in the x axis direction

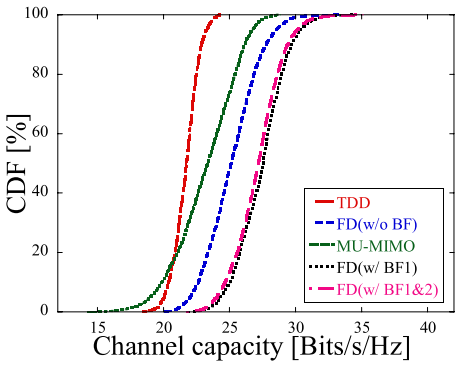

(b)Array facing in the y axis direction

Fig. 7 CDF of channel capacity between B-C.

downlink and uplink users, and the signal flow direction is reversed. $C_{2\mathrm{BF}}$ and $C_{1\mathrm{i}}$ are the capacities when the uplink and downlink users are switched, and the system capacity is defined as the sum of them. Therefore, the total system capacity of the proposed FD is defined as (20) because this study assumes the uplink and downlink periods are assigned equally.

4.3 Transmission Capacity Characteristics when UT2 is Placed at Point C

Figures 6 and 7 show the Cumulative Distribution Function (CDF) of the transmission capacity of the various communication methods discussed in 3, where UT2 is placed at point C, UT1 moved between A and B, and then between B and C. In this arrangement, UT2 and BS lie on the same line from UT1. This means the capacity of the proposed FD is likely to be worst since the desired signals from UT1 to BS are also suppressed by null-beamforming to UT2. TDD, MU-MIMO, and FD represent the channel capacities of TDD, multi-user MIMO, and FD MIMO. The terms w/o BF, w/ BF1, and w/ BF1&2 stand for the channel capacities when the value of L in equations (16)–(19) is 0, 1 and 2, respectively. These results confirm that in both cases the FD scheme outperforms TDD and MU-MIMO schemes. Of particular interest in Fig. 6(a), FD with beamforming (w/ BF1 and w/ BF1&2) yields better performance than FD without beamforming (w/o BF), and FD (w/ BF1) improves the median value of the transmission capacity by 14.4 and 7.19 Bits/s/Hz compared to that of TDD and MU-MIMO, respectively, when the terminal antennas are co-linear on the x axis direction and UT1 is located between A and B. On the other hand, the advantage of the FD scheme compared to TDD and MU-MIMO schemes is small in Fig. 7, as UT1 lies between B and C, i.e. the distance between the two UTs is quite short, i.e. the interference is not sufficiently suppressed. Nevertheless, Fig. 7(b) shows FD with beamforming (w/ BF1 and w/ BF1&2) yields better performance than all other schemes including FD without beamforming (w/o BF) when both UT arrays are face the y axis direction. The curve, FD (w/ BF1), plotted in Fig. 7(b) shows an improvement in the median value of the transmission capacity by 5.79 and 4.19 Bits/s/Hz compared to TDD and MU-MIMO, respectively. This is because the first eigenvalue in the interference channel becomes large compared to the other eigenvalues, and this condition suits the beamforming technique. These results confirm that high performance is attained when the two UTs operate in end-fire orientation.

4.4 Transmission Capacity Characteristics when UT2 is Placed at Point D

Figures 8 and 9 plots the CDF of the transmission capacity of the various communication methods, where UT2 is placed at point D, and UT1 moves between A and B, and then between B and C. In this case, the directions of the users as

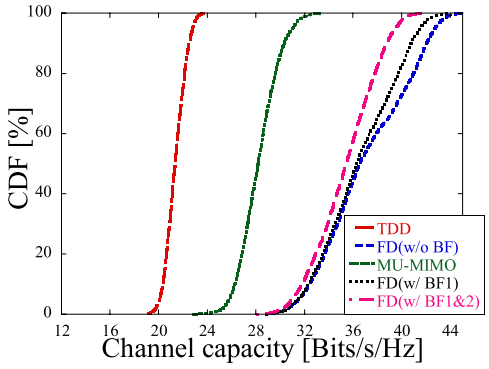

(a)Array facing in the x axis direction

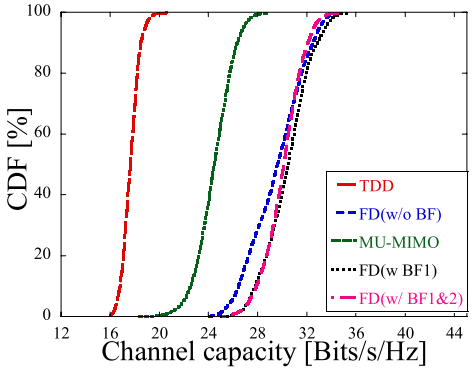

(b)Array facing in the y axis direction

Fig. 8 CDF of channel capacity between A-B.

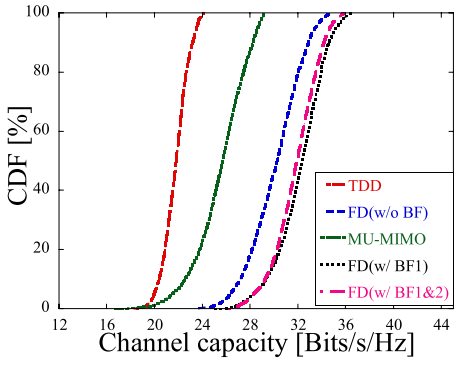

(a)Array facing in the x axis direction

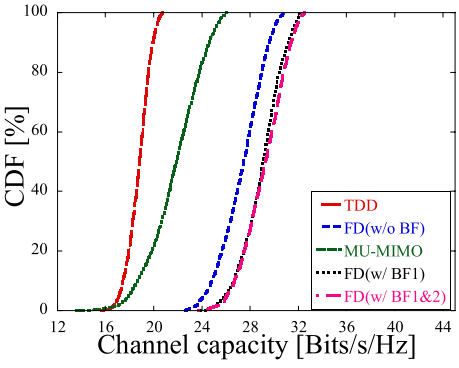

(b)Array facing in the y axis direction

Fig. 9 CDF of channel capacity between B-C.

seen from the BS are different, so BD-based MU-MIMO is expected to offer better performance than that demonstrated in Figs. 6 and 7. The inter-user direction with respect to the array orientation varies depending on UT1 location, and this is the cause of the great performance variation in the proposed scheme shown in Fig. 8. The performance variation can be understood from the spread of CDF in Fig. 8. Nevertheless, from the results shown in Fig. 8, the curve, FD (w/o BF), shown in Fig. 8(a) realizes higher channel capacity than the conventional method as in 4.3, and improves the median value of the transmission capacity by 15.2 and 8.36 Bits/s/Hz compared to that of TDD and MU-MIMO, respectively. Similarly, when UT1 is located between B and C where the terminal antennas are co-linear in the x axis direction, the curve, FD (w/ BF2), shown in Fig. 9(b) realizes higher channel capacity than the conventional methods, and improves the median value of the transmission capacity by 10.5 and 7.39 Bits/s/Hz compared to that of TDD and MU-MIMO, respectively. Both antenna arrangements improve the capacity of the FD MIMO communication system by up to 2.1 Bits/s/Hz even if just a single-null is used. The measurements reveal that eigen-beamforming attains superior performance even when the inter-terminal distance is small and the interference power is large.

5. Conclusion

This paper introduced an inter-terminal interference suppression method for a FD MIMO communication system, where uplink and downlink users are simultaneously active. For interference suppression, the transmitting user employs the eigen-beamforming method. A field measurement campaign showed that the FD MIMO communication scheme offers larger transmission capacity than the conventional schemes regardless of the inter-user distance. The measurement results showed the proposed scheme improved the median value of the transmission capacity from 1.30 to 1.53 times over that of the conventional TDD and MU-MIMO schemes in the scenario considered.

Acknowledgments

This research and development work was supported by the MIC/SCOPE (155002002).

References

[1] S. Hong, J. Brand, J. Choi, M. Jain, J. Mehlman, S. Katti, and P. Levis, "Applications of self-Interference cancellation in 5G and beyond," IEEE Commun. Mag., vol.52, no.2, pp.114–121, Feb. 2014.
[2] J. Choi, M. Jain, K. Srinivasan, P. Levis, and S. Katti, "Achieving single channel, full duplex wireless communication," MobiCom'10, pp.1–12, ACM, Sept. 2010.

[3] E. Aryafar, M.A. Khojastepour, K. Sundaresan, S. Rangarajan, and M. Chiang, "MIDU: Enabling MIMO full duplex," MobiCom'12, pp.257–268, ACM, Aug. 2012.
[4] M. Duarte and A. Sabharwal, "Full-duplex wireless communications using off-the shelf radios: Feasibility and first results," Forty Fourth Asilomar Conf. Sig., Systems, and Components, Nov. 2010.
[5] D. Bharadia, S. Katti, "Full duplex MIMO radios," Proc. 11th USENIX Symp. NSDI, pp.359–372, April 2014.
[6] H. Ju and R. Zhang, "Optimal resource allocation in full-duplex wireless-powered communication network," IEEE Trans. Commun., vol.62, no.10, pp.3528–3540, Oct. 2014.
[7] M. Jainy, J.I. Choi, T.M. Kim, D. Bharadia, S. Seth, K. Srinivasan, P. Levis, S. Katti, and P. Sinha, "Practical, real-time, full duplex wireless," MobiCom'11, pp.301–312, ACM, Sept. 2011.
[8] M. Tsunezawa, N. Honma, K. Takahashi, K. Murata, and K. Nishimori, "Experimental evaluation of inter-array decoupling technique suitable for MIMO full-duplex system," Int. Symp. Antennas and Propagat. (ISAP), pp.24–28, Oct. 2016.
[9] T. Ohto, K. Yamamoto, K. Haneda, T. Nishino, and M. Morikura, "Generalized PF scheduling for bidirectional and user-multiplexing unidirectional full-duplex links," Proc. IEEE 2015 21st Asia-Pacific Conf. Commun. (APCC), pp.359–369, Oct. 2015.
[10] S. Vishwanath, N. Jindal, and A. Goldsmith, "Duality, achievable rates, and sum-rate capacity of gaussian MIMO broadcast channels," IEEE Trans. Inf. Theory, vol.49, no.10, pp.2658–2668, Oct. 2003.
[11] K.K. Wong, R.D. Murch, and K.B. Letaief, "A joint-channel diagonalization for multiuser MIMO antenna systems," IEEE Trans. Wireless Commun., vol.2, no.4, pp.773–786, July 2003.
[12] Q.H. Spencer, A.L. Swindlehurst, and M. Haardt, "Zero forcing methods for downlink spatial multiplexing in multiuser MIMO channels," IEEE Trans. Signal Process., vol.52, no.2, pp.461–471, Feb. 2004.
[13] R.S. Blum, "MIMO capacity with interference," IEEE J. Sel. Areas Commun., vol.21, no.5, pp.793–801, June 2003.

Appendix: The Weight Determination by BD Method

The weight is determined by BD method for MU-MIMO scheme, but the total number of the antennas at the UT side is larger than that at the BS. This means the normal BD method cannot be simply applied to this case. First, we consider downlink channel $\boldsymbol{H}_2$ in Fig. 1. The number of antennas at all stations are identically given as $M = 4$. Therefore, singular value decomposition of $\boldsymbol{H}_2$ defined by (2)–(6) is written as,

$$\boldsymbol{H_2} = [\boldsymbol{u}_{2,1}, \cdots, \boldsymbol{u}_{2,4}]\boldsymbol{\Sigma_2}[\boldsymbol{v}_{2,1}, \cdots, \boldsymbol{v}_{2,4}]^H. \quad (\text{A}\cdot 1)$$

Also, we select the highest two eigen-modes out of four modes, and the eigenvectors, $\boldsymbol{u}_{2,1}$ and $\boldsymbol{u}_{2,2}$, corresponding to the selected eigen-modes are used as the receiving weights. Therefore, the downlink channel with mode selection is defined as,

$$\boldsymbol{H_{2d}} = [\boldsymbol{u}_{2,1}, \boldsymbol{u}_{2,2}]^{\mathrm{H}}\boldsymbol{H}_2. \quad (\text{A}\cdot 2)$$

We perform same processing for ${\boldsymbol{H}_1}^T$ and calculate $\boldsymbol{H}_{1\mathrm{d}}$. By using this mode selection technique, the total number of the equivalent antennas at UT side is four, which is exactly same to the number of the antennas at BS. Therefore, the BD method can be applicable for this scenario.

Yuta Kashino received the B.E. in electrical and electronic engineering from Iwate University, Morioka, Japan in 2016. He is currently in the master program in Iwate University. His research interest is interference reduction techniques for MIMO full-duplex communication.

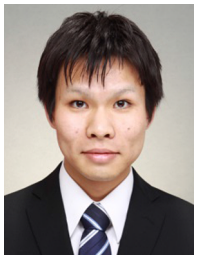

Masakuni Tsunezawa received the B.E. in electrical and electronic engineering from Iwate University, Morioka, Japan in 2015. He is currently in the master program in Iwate University. His research interest is interference reduction techniques for MIMO full-duplex communication.

Naoki Honma received the B.E., M.E., and Ph.D. degrees in electrical engineering from Tohoku University, Sendai, Japan in 1996, 1998, and 2005, respectively. In 1998, he joined the NTT Radio Communication Systems Laboratories, Nippon Telegraph and Telephone Corporation (NTT), in Japan. He is now working for Iwate University. He received the Young Engineers Award from the IEICE of Japan in 2003, the APMC Best Paper Award in 2003, the Best Paper Award of IEICE Communication Society in 2006, and 2014 Asia-Pacific Microwave Conference Prize in 2014, respectively. His current research interest is MIMO system and its applications. He is a member of IEEE.

Kentaro Nishimori received the B.E., M.E. and Ph.D. degrees in electrical and computer engineering form Nagoya Institute of Technology, Nagoya, Japan in 1994, 1996 and 2003, respectively. In 1996, he joined the NTT Wireless Systems Laboratories, Nippon Telegraph and Telephone Corporation (NTT), in Japan. He was senior research engineer on NTT Network Innovation Laboratories. He is now associate professor in Niigata University. He was a visiting researcher at the Center for Teleinfrastructure (CTIF), Aalborg University, Aalborg, Denmark from Feb. 2006 to Jan. 2007. He was an Associate Editor for the Transactions on Communications for the IEICE Communications Society from May 2007 to May 2010 and Assistant Secretary of Technical Committee on Antennas and Propagation of IEICE from June 2008 to May 2010. He is now Secretary of Technical Committee on Antennas and Propagation of IEICE. He received the Young Engineers Award from the IEICE of Japan in 2001, Young Engineer Award from IEEE AP-S Japan Chapter in 2001, Best Paper Award of Software Radio Society in 2007. He received IEICE Best Paper Award in 2010. His main interests are spatial signal processing including MIMO systems and interference management techniques. He is a member of IEEE and IEICE.